Microbiology (2010), **156**, 3734–3743 **DOI** 10.1099/mic.0.042192-0

Arginine metabolism in *Trichomonas vaginalis* infected with *Mycoplasma hominis*

Mary Morada,[1] Mafruha Manzur,[1] Brian Lam,[1,2] Cho Tan,[1,2] Jan Tachezy,[3] Paola Rappelli,[4] Daniele Dessì,[4] Pier L. Fiori[4]† and Nigel Yarlett[1,2]†

Correspondence
Nigel Yarlett
nyarlett@pace.edu

[1]Haskins Laboratories, Pace University, NY 10038, USA

[2]The Department of Chemistry and Physical Sciences, Pace University, NY 10038, USA

[3]Department of Parasitology, Charles University, Prague, Czech Republic

[4]Department of Biomedical Sciences, Division of Experimental and Clinical Microbiology, University of Sassari, 07100 Sassari, Italy

Both *Mycoplasma hominis* and *Trichomonas vaginalis* utilize arginine as an energy source via the arginine dihydrolase (ADH) pathway. It has been previously demonstrated that *M. hominis* forms a stable intracellular relationship with *T. vaginalis*; hence, in this study we examined the interaction of two localized ADH pathways by comparing *T. vaginalis* strain SS22 with the laboratory-generated *T. vaginalis* strain SS22-MOZ2 infected with *M. hominis* MOZ2. The presence of *M. hominis* resulted in an approximately 16-fold increase in intracellular ornithine and a threefold increase in putrescine, compared with control *T. vaginalis* cultures. No change in the activity of enzymes of the ADH pathway could be demonstrated in SS22-MOZ2 compared with the parent SS22, and the increased production of ornithine could be attributed to the presence of *M. hominis*. Using metabolic flow analysis it was determined that the elasticity of enzymes of the ADH pathway in SS22-MOZ2 was unchanged compared with the parent SS22; however, the elasticity of ornithine decarboxylase (ODC) in SS22 was small, and it was doubled in SS22-MOZ2 cells. The potential benefit of this relationship to both *T. vaginalis* and *M. hominis* is discussed.

Received 4 June 2010
Revised 9 July 2010
Accepted 21 July 2010

INTRODUCTION

The arginine dihydrolase (ADH) pathway catalyses the conversion of arginine to ornithine and ammonia via the enzymes arginine deiminase (ADI), catabolic ornithine carbamyltransferase (cOCT) and carbamate kinase (CK) (Fig. 1). Cumulatively, the pathway removes nitrogen from amino acids with the generation of ATP, performing a function analogous to that of the urea cycle of vertebrates. The ADH pathway is present in some protists such as *Trichomonas vaginalis* (Linstead & Cranshaw, 1983) and *Giardia intestinalis* (Schofield *et al.*, 1990), as well as some Gram-positive (*Streptococcus* spp.; Griswold *et al.*, 2004) and Gram-negative bacteria (*Pseudomonas* spp.; Lu *et al.*, 2004), and some Mollicutes (*Mycoplasma hominis*, *Mycoplasma arginini*; Fenske & Kenny, 1976; Das *et al.*, 2004), in which it has been proposed to function as an alternative ATP-generating mechanism. The *Giardia lamblia* ADI is proposed to have multiple functions, including a peptidylarginine deiminase that converts protein bound arginine to citrulline (Touz *et al.*, 2008). No such activity has been demonstrated for *T. vaginalis*, in which the pathway is proposed to function solely for energy generation, contributing about 10 % of the total energy requirements (Yarlett *et al.*, 1996). In *T. vaginalis*, the first and rate-limiting enzyme, ADI, is localized to a subcellular fraction, possibly the hydrogenosome, whereas the other enzymes of the pathway are present in the cytoplasmic fraction (Yarlett *et al.*, 1994).

T. vaginalis and several *Mycoplasma* species (*M. hominis*, *Mycoplasma genitalium*, *Ureaplasma urealyticum*) are common urogenital parasites of vertebrates. In addition, *M. hominis* is commonly found as an intracellular parasite of *T. vaginalis* (Rappelli *et al.*, 1998; Dessì *et al.*, 2005), but not of *Tritrichomonas foetus* (Dessì *et al.*, 2005). In a study of 35 patients with trichomoniasis, *M. hominis* was isolated from 33 patients by *in vitro* culture of *T. vaginalis*; no other *Mycoplasma* species was detected (Dessì *et al.*, 2005). The exact nature of this intimate relationship between *T. vaginalis* and *M. hominis* is unknown, but it has been proposed to be saprophytic (Rappelli *et al.*, 1998). This

†These authors contributed equally to this work.

Abbreviations: ADH, arginine dihydrolase; ADI, arginine deiminase; aOCT, anabolic ornithine carbamyltransferase; CK, carbamate kinase; cOCT, catabolic ornithine carbamyltransferase; OAT, ornithine aminotransferase; OCT, ornithine carbamyltransferase; ODC, ornithine decarboxylase.

Two supplementary figures and two supplementary tables are available with the online version of this paper.

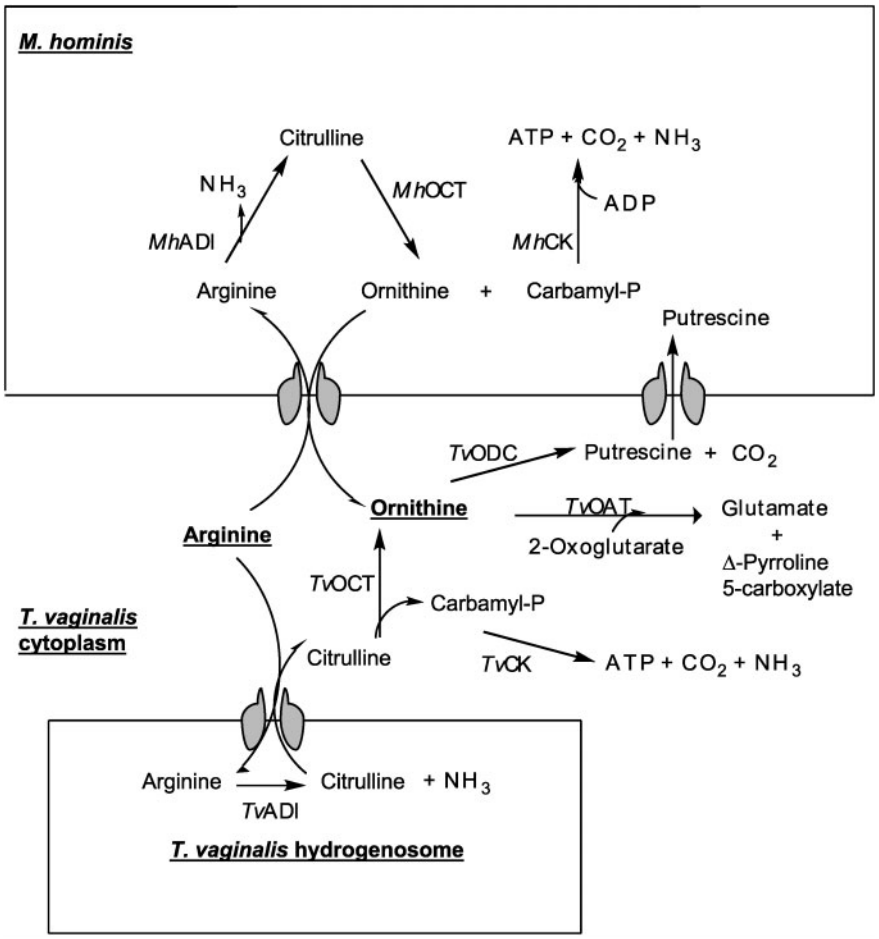

Fig. 1. Enzymes of the ADH pathway. Enzyme reactions that occur in the hydrogenosome are indicated in the lower box; enzyme reactions that occur in the intracellular *M. hominis* are indicated in the upper box. *M. hominis* and *T. vaginalis* enzymes are prefixed *Mh* and *Tv*, respectively.

study attempts to clarify the metabolism of arginine in *T. vaginalis* infected with *M. hominis*, and to determine whether this relationship benefits *T. vaginalis* and/or *M. hominis*.

METHODS

Cultures. *T. vaginalis* SS22, *T. vaginalis* infected with *M. hominis* (SS22-MOZ2) and *M. hominis* (MOZ2) were cultured in tryptose–yeast extract–maltose medium supplemented with 10 % horse serum (Diamond, 1957). The presence of *M. hominis* in *T. vaginalis* SS22-MOZ2 was detected by PCR using the primers RNAH1 and RNAH2 for *M. hominis* (Blanchard *et al.*, 1993), as previously described (Rappelli *et al.*, 1998). The isogenic strain SS22-MOZ2 was obtained by infecting SS22 with *M. hominis* (MOZ2) isolated from a naturally occurring *T. vaginalis* strain, MPM-02, infected with *M. hominis*. Briefly, *T. vaginalis* MPM-02 was harvested during exponential growth by centrifugation at 350 ***g***, and the supernatant was filtered through a 0.45 μm pore-size filter membrane. An aliquot of filtered supernatant containing 10^6 (calculated as c.f.u.) mycoplasma was added to a 10 ml culture of *T. vaginalis* SS22. Identical bacterial suspensions were inoculated both on 10 ml fresh Diamond's medium (Diamond, 1957) and on 10 ml *T. vaginalis*-conditioned medium (obtained from a filtered overnight culture of mycoplasma-free SS22). All samples were then daily passaged with 1 : 16 dilution for 30 days. Exponential-phase cells were harvested at 4000 ***g*** for 10 min at 4 °C in a Sorvall RC-2B centrifuge (DuPont) and washed in a buffer containing 30 mM sodium phosphate, 74 mM sodium chloride, 0.6 mM calcium chloride and 1.6 mM potassium chloride, pH 7.4. Washed cells were resuspended in 225 mM sucrose–10 mM Tris isotonic buffer, pH 7.4.

Subcellular fractionation. Concentrated cell pellets were broken by 35 strokes in a Potter–Elvehjem tissue homogenizer at 4 °C. The broken cells were diluted with 225 mM sucrose–10 mM Tris, pH 7.4, containing 1 mM calcium chloride and 1 mM magnesium chloride, and centrifuged successively at 400 ***g*** for 10 min, 2200 ***g*** for 10 min and 28 000 ***g*** for 30 min, yielding nuclear-enriched, hydrogenosome-enriched and lysosome-enriched pellets, respectively.

Density-gradient centrifugation. Self-generating gradients were prepared using 50 % (w/v) Percoll containing 225 mM sucrose–10 mM Tris, pH 7.4, 1 mM calcium chloride and 1 mM magnesium chloride. Fractions (1 ml, 12–18 mg protein) were layered onto 10 ml Percoll mixture and centrifuged at 46 000 ***g*** for 45 min at 4 °C in a 6 × 12 ml swing-out rotor (Beckman OTD 95). Fractions were

collected by removing 1 ml aliquots. The density of fractions was calculated from determining the weight of 1 ml volumes. Chemicals and reagents were supplied by Sigma.

For enzyme analysis, *T. vaginalis* SS22, SS22-MOZ2 and *M. hominis* MOZ2 were cultured as described above in 1 l of medium. Cells were harvested by centrifugation at 5000 ***g*** for 10 min, washed twice in PBS, and resuspended in 10 mM phosphate buffer, pH 7.4, containing 1 mg each of aprotinin, leupeptin and *N*-α-tosyl-L-lysinyl-chloromethylketone (TLCK) ml^{-1}. Cells were stored at −70 °C until used.

Enzyme assays. The integrity of the organelles was confirmed by performing all enzyme assays in isotonic buffered solutions (225 mM sucrose), to which 0.05 % Triton X-100 was added to demonstrate latency of activity. ADI (EC 3.5.3.6) was determined by measuring the colorimetric formation of citrulline at 37 °C. The assay contained 0.5–2.5 mM L-arginine, 40 mM MES, pH 8.0, and 0.07 mg protein in a final volume of 1.0 ml. After 30 min, the reaction was stopped by the addition of 0.075 ml 100 % (w/v) TCA, and the citrulline formed determined using diacetyl monoxime, as described by Boyde & Rahmatullah (1980). cOCT (EC 2.1.3.3) was determined by measuring $^{14}CO_2$ release from L-[^{14}C-carbamyl] citrulline. The reaction mixture contained 40 mM Tricine, pH 6.0, 0.1 mM L-citrulline, 0.1–1.0 mM L-[^{14}C-carbamyl] citrulline [57.7 mCi $mmol^{-1}$ (2135 MBq $mmol^{-1}$)] (DuPont, N.E.N. Research Products) and 0.07 mg protein in a final volume of 1 ml. After incubation at 37 °C for 1 h, the reaction was stopped with 1 ml 40 % TCA and incubated for a further 30 min, and the CO_2 was trapped using benzethonium hydroxide-soaked filter paper. In the anabolic direction, anabolic ornithine carbamyltransferase (aOCT) was determined by measuring citrulline formation with 10 mM ornithine in 0.1 M Tris buffer, pH 8.0, and 0.07 mg protein; the reaction was started by the addition of 10 mM carbamyl phosphate and incubated for 15 min at 37 °C. The reaction was stopped by the addition of 6 % TCA, and the amount of citrulline formed was determined as described by Boyde & Rahmatullah (1980). CK (EC 2.7.2.2) activity was determined in incubations containing 0.1–1.0 mM ADP, 20 mM $MgSO_4$, 0.15 mM luciferin, 1 mg firefly lantern extract and 1 mM carbamyl phosphate, in 50 mM potassium phosphate buffer, pH 7.6. ATP formation was determined by monitoring luminescence using a photomultiplier tube. Ornithine decarboxylase (ODC; EC 4.1.1.17) was determined by measuring the release of $^{14}CO_2$ from 0.05–1.0 mM 1-[^{14}C]ornithine [42.5 mCi $mmol^{-1}$ (1602.25 MBq $mmol^{-1}$)] in 0.1 M acetate buffer, pH 6.5, containing 60 μM pyridoxal phosphate, as previously described (Yarlett *et al.*, 1993). Malic enzyme (EC 1.1.1.39) was assayed using 6 mM triethanolamine, pH 6.8, containing 1 mM NAD, 0.66 mM $MnCl_2$ and 0.1 % Triton X-100; the change at A_{340} was monitored upon the addition of 33 mM neutralized sodium malate (Dolezal *et al.*, 2004). Determination of the pH optima of enzyme activities was performed using the above assay methods with pHs varying from 5.0 to 7.5 with 40 mM MES (pK_a 6.15 at 20 °C) and from 7.0 to 9.0 with 40 mM HEPPS (pK_a 8.0 at 20 °C). Protein concentrations were determined using the Lowry method.

HPLC. The intracellular and extracellular amine content of *T. vaginalis* SS22, SS22-MOZ2 and *M. hominis* MOZ2 was determined by centrifugation of 24 h cultures at 5000 ***g*** for 10 min. Pellets were washed once with PBS, pH 7.4, and proteins removed by addition of 6 % TCA. Culture medium was mixed with 10 % (v/v) of 60 % TCA. Samples were microfuged at 14 000 ***g*** for 1 min, and amines were separated by reverse-phase HPLC using a series LC 410 pump (Perkin–Elmer) coupled to a C-18 10 μm particle size column (4.5 × 250 mm) at a flow rate of 1 ml min^{-1}. The method employed a 70 min discontinuous gradient starting with 90 % (v/v) buffer A: 0.1 M sodium phosphate monobasic, pH 2.65, containing 8 mM octane sulfonic acid and 0.05 mM EDTA. Buffer B consisted of HPLC grade acetonitrile. Separation of amines used a 35 min discontinuous gradient switching to 80 % A at 15 min and 60 % A at 25 min, followed by a 10 min recycle time to regenerate the start conditions. Standards and samples were post-column derivatized by mixing with two parts 1.5 mM *o*-phthalaldehyde dissolved in 3 ml methanol and made up to 1 l with 0.5 M boric acid containing 0.43 M KOH and 0.014 M 2-mercaptoethanol, pH 10.4. The derivatized compounds were analysed using a fluorescence monitor (λ_{excit} 320 nm, λ_{em} 455 nm). Areas under the peaks were determined using β-RAM computer software (IN/US Systems), version 1.62.

Enzyme kinetics. Kinetic analysis of the ADH pathway in *T. vaginalis* SS22, SS22-MOZ2 and *M. hominis* MOZ2 was performed by varying the substrate for each enzyme and measuring the rate of product formation. K_m and V_{max} values were determined from straight-line Hanes–Woolf plots ($[S]/v$ versus $[S]$). The specificity constant V/K_m is derived from the initial slope of the graph of velocity versus substrate concentration for a reaction that obeys the Michaelis–Menten equation (Cornish-Bowden, 2004). This constant is therefore the second-order rate constant for the reaction at low substrate concentration, which is typically true for intracellular environments where substrate concentrations are below the K_m concentration. The elasticity (ε), which is defined as the fractional change in rate of the enzyme for a fractional change in substrate concentration, was determined for each enzyme in the pathway from a plot of $\log(v)$ versus $\log[S]$ (Fell, 1997). The intracellular concentration around which the elasticity was required was determined by HPLC of the intracellular amine concentration and the ν at this substrate concentration determined from the Hanes–Woolf plot. The enzyme elasticity was calculated from the slope of the double log plot ranging from 95 % of $[S]$ to 105 % of $[S]$. Using the connectivity theorem ($C^J_{enz1}\bullet\varepsilon^{enz1}_{s1} + C^J_{enz2}\bullet\varepsilon^{enz2}_{s2} = 0$), it is possible to express the ratio of the flux control coefficients for pairs of enzymes in the pathway under different conditions ($C^J_{enz1}/C^J_{enz2} = \varepsilon^{enz2}_{s2}/\varepsilon^{enz1}_{s1}$).

Bioinformatic analyses. The amino acid sequence of *G. intestinalis* (strain WB) ADI (accession no. XP_001705755) was used as the query for a BLAST search in the *T. vaginalis* (strain G3) genome database of Eukaryotic Pathogen Database Resources (http://eupathdb.org/eupathdb/). Three sequences with significant similarity to *G. intestinalis* ADI (TVAG_467820, TVAG_344520 and TVAG_183850) were aligned with *M. hominis* (accession no. D13314 0.1) and *M. arginini* (accession no. CAA38210) using CLUSTAL_X (Thompson *et al.*, 1997) and manually edited with BioEdit software (Hall, 1999). Putative mitochondrial targeting sequences and cellular localization were predicted using the program PSORT II (http://psort.hgc.jp/).

Quantitative RT-PCR (RT-qPCR) of ADI. To determine whether the elevated ADI activity in *T. vaginalis* SS22-MOZ2 compared with the parent SS22 was related to the additive effect of intracellular *M. hominis* or to upregulation of expression of *T. vaginalis* ADI, an RT-qPCR was designed to compare the mRNA expression of all three ADIs identified in the *T. vaginalis* genomic library. The three sets of primers were designed on the basis of sequence differences between *M. hominis* and *T. vaginalis* ADI. In particular, we used the following pairs of primers: TvADI 423-cDNA-92185, Tv92185F (5′-TTCGTCCAACCTTCAACTCAAGAAG-3′) and Tv92185R (5′-CTTTATCTGGATCTGGTGGTTTTTCATAG-3′), amplicon length 111 bp; TvADI-485-cDNA-96423, Tv96423F (5′-CGCGCATCATCAAGTTTTCGC-3′) and Tv96423R (5′-CTTTTTGGGATTCGGTGGGTGC-3′), amplicon length 119 bp; TvADI-185-cDNA-86485, Tv86485F (5′-GCTCTGTTCAATTCAACGCAG-3′) and Tv86485R (5′-GAATTGTGTGGCAGCTGTTGGTGG-3′), amplicon length 82 bp. These sequences were used to probe the *M. hominis*-infected (SS22-MOZ2) and -uninfected (SS22) strains of *T. vaginalis*. Results were compared with the expression of the actin gene (housekeeping gene) in *M. hominis*-infected and -uninfected *T. vaginalis*. RNA from cells was harvested by centrifugation and extracted with TRIzol reagent (Invitrogen), followed by double DNase I digestion for subsequent RT-qPCR with specific primers. Relative gene expression was calculated by the

$2^{-\Delta\Delta Ct}$ method, by using actin as housekeeping gene. Experiments were performed in triplicate, and variation in gene expression was quantified by calculating $2^{-\Delta\Delta Ct}$ *M. hominis*-infected *T. vaginalis*/$2^{-\Delta\Delta Ct}$: *M. hominis*-uninfected *T. vaginalis* ratios. The expression of all ADI genes was evaluated in triplicate in three different experiments.

RESULTS

Enzyme activities and metabolic flow through the ADH pathway of *T. vaginalis* with and without *M. hominis*

We have previously observed significant variations in the activities of the ADH enzymes, particularly ADI and cOCT, between different strains of *T. vaginalis*, and that was borne out by the variations in enzyme activities observed for strain SS22 in this study and by earlier data with strain C1 (Table 1 and Supplementary Table S1). The parent mycoplasma-free *T. vaginalis* strain (SS22) was infected *in vitro* with *M. hominis* (MOZ2), isolated from a naturally occurring *T. vaginalis* isolate, MPM02, infected with *M. hominis* (MOZ2) (Dessì *et al.*, 2005). Typically, about 5–10 mycoplasma were observed in these strains (Fig. 2). Whole-cell extracts prepared from *T. vaginalis* SS22, *T. vaginalis* infected with *M. hominis* SS22-MOZ2 and *M. hominis* MOZ2 were examined for the kinetic properties of the enzymes of the ADH pathway. The enzymes ornithine carbamyltransferase (OCT), CK and ODC demonstrated minimal differences in kinetic properties between *T. vaginalis* infected with *M. hominis* SS22-MOZ2 and the parent uninfected *T. vaginalis* SS22 (Table 1). In contrast, the first and rate-limiting enzyme of the ADH pathway, ADI, demonstrated significant differences in V_{max} (Table 1). The *T. vaginalis* infected with *M. hominis* SS22-MOZ2 had an average sixfold increased V_{max} compared with the uninfected parent SS22 (Table 1). Overall, the *T. vaginalis* strain SS22-MOZ2 had a 19-fold increased specificity (V_{max}/K_m) for ADI compared with the parent strain SS22. The kinetic constants for ADI of *M. hominis* (MOZ2) indicated that the V_{max} and K_m for ADI were similar to those obtained for *T. vaginalis* strain SS22-MOZ2, suggesting that the increased specificity for this enzyme was the result of the presence of *M. hominis*. Kinetic analysis of ADH enzymes from *M. hominis* revealed that the specificity of ADI was 23-fold greater than that for *T. vaginalis* SS22; likewise, kinetic analysis of cOCT revealed a 227-fold greater specificity than that of *T. vaginalis* strain SS22 (Table 1); however, the ATP-forming enzyme CK was fivefold more efficient in *T. vaginalis* SS22 compared with *M. hominis* (Table 1). The combination of both ADH pathways in *T. vaginalis* SS22-MOZ2 had a higher overall specificity for conversion of arginine to ATP and ornithine, which may be beneficial to *T. vaginalis* and *M. hominis*. The elasticity (ε) of the enzymes of the pathway was determined using metabolic flow analysis (Fell, 1997). The only enzyme of the pathway with increased specificity was ODC (Table 2).

The pH optima of the enzymes from *T. vaginalis* SS22 and SS22-MOZ2 were compared with those of *M. hominis* (Supplementary Fig. S1). The optimum pH for cOCT was 6.0 for SS22, SS22-MOZ2 and MOZ2; however, aOCT was found to have an optimal pH of 7.0 for MOZ2 and 8.0 for *T. vaginalis* SS-22 and SS22-MOZ2. By comparison, ADI was found to have an optimal pH of 6.5 for *M. hominis* MOZ2 and *T. vaginalis* SS22-MOZ2, whereas the parent uninfected *T. vaginalis* SS22 had an optimal pH of 8.0 for ADI, further supporting the view that the *M. hominis* ADI is responsible for the enhanced ADI kinetics in *T. vaginalis* SS22-MOZ2.

ADI-coding genes and localization of the gene products in *T. vaginalis*

A BLAST search of the *T. vaginalis* genome database revealed the presence of three copies of the ADI gene (TvADI-1, TvADI-2 and TvADI-3) encoding proteins with a calculated molecular mass of 46 000–47 000 Da. Alignment with *M. arginini*, for which a crystal structure has been determined (Das *et al.*, 2004), revealed the presence of conserved residues involved in substrate binding and/or the enzyme active site (Fig. 3). The positional equivalent of the catalytic triad Cys397, His268, Glu213 determined in *M. arginini* ADI (Das *et al.*, 2004) is conserved in TvADI-1

Table 1. Kinetic properties of ADH enzymes in the parent *T. vaginalis* SS22, *T. vaginalis* infected with *M. hominis* (SS22-MOZ2) and *M. hominis* MOZ2

Enzyme assays were performed as described in Methods using whole-cell extracts. V_{max} is expressed as μM min^{-1} using 1 mg protein. The V_{max} and K_m values are expressed as mean ± SD for four determinations. ND, Not detected.

Enzyme	*T. vaginalis* SS22			*T. vaginalis* SS22-MOZ2			*M. hominis*		
	V_{max} (μM min^{-1})	K_m (μM)	V_{max}/K_m	V_{max} (μM min^{-1})	K_m (μM)	V_{max}/K_m	V_{max} (μM min^{-1})	K_m (μM)	V_{max}/K_m
ADI	76.6 ± 7.4	200 ± 36	0.38	433 ± 14.0	60 ± 10	7.2	516 ± 24	60 ± 7.1	8.6
cOCT	40.1 ± 4.5	138 ± 18	0.29	48.0 ± 12.1	125 ± 23	0.38	11864 ± 432	180 ± 12	65.9
aOCT	1938 ± 210	3400 ± 170	0.57	1624 ± 180	2900 ± 240	0.56	75964 ± 9258	4200 ± 295	18.1
CK	3900 ± 480	60 ± 3.8	65.0	4274 ± 390.	83 ± 12.0	51.5	1274 ± 94	95 ± 12	13.4
ODC	1.10 ± 0.2	18 ± 3.0	0.06	1.15 ± 0.3	16 ± 2.0	0.07	ND	ND	–

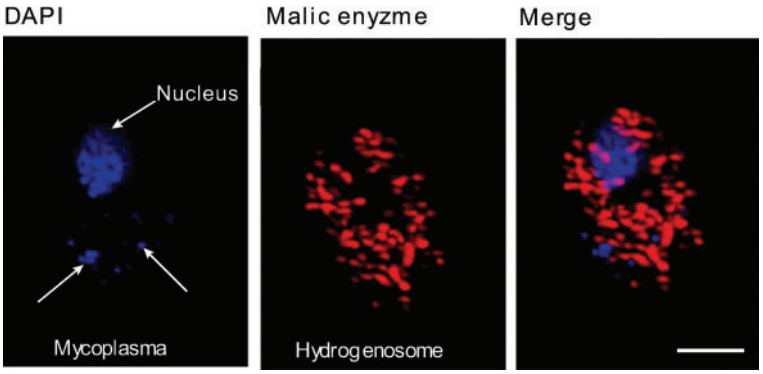

Fig. 2. *M. hominis* in experimentally infected *T. vaginalis* strain SS22-MOZ 2. *M. hominis* was visualized by DNA staining using 4′,6-diamidino-2-phenylindole (DAPI; blue). Hydrogenosomes were stained for malic enzyme using rabbit polyclonal anti-malic enzyme antibody and Alexa Fluor 546-conjugated donkey anti-rabbit immunoglobulin (red). Bar, 10 μm.

(Cys408, His283, Glu230) and TvADI-2 (Cys405, His281, Glu228), while Cys405 is replaced by Ser405 in TvADI-3.

All three putative TvADI sequences contained a mitochondrion-like N-terminal targeting presequence with a predicted cleavage site for a processing peptidase (Fig. 3), and a high probability of mitochondrial localization estimated by PSORT II (56–65 %) and TargetP (mTP values 0.500–0.710). These predictions suggested the localization of ADI in *T. vaginalis* hydrogenosomes, an anaerobic form of mitochondria in these parasites. The *T. vaginalis* ADI sequences group within the Eukaryota, suggesting that the ADI-encoding genes were present in a common ancestor, which does not support horizontal gene transfer from a prokaryotic source (Supplementary Fig. S2).

Kinetics of ADI in hydrogenosomal fractions from *M. hominis*-infected and -uninfected *T. vaginalis*

Subcellular fractionation of *T. vaginalis* SS22 and the *M. hominis*-infected SS22-MOZ2 had typical distribution profiles for hydrogenosomes based upon the data for malic enzyme, a marker enzyme for the organelle (Fig. 4a, b). The relative specific activity plot for ADI mirrored that for malic enzyme in extracts prepared from SS22 (Fig. 4c). However, the SS22-MOZ2 fractions typically had a second band of ADI activity which co-sedimented with the nuclear fraction, suggesting that *M. hominis* sediments with the nuclei and only minor contamination of the hydrogenosome fraction occurred (Fig. 4d). OCT, which in aerobic eukaryotes localizes to the mitochondrion, was found predominantly in the non-sedimentable fraction in both SS22 and SS22-MOZ2 (Fig. 4e, f). Kinetic analysis of ADI using the hydrogenosome-enriched fractions from *T. vaginalis* SS22 and SS22-MOZ2 revealed minimal differences in the V_{max} (65.8 ± 1.2 and 79.8 ± 2.8 μM min^{-1}, respectively) and K_m (180 ± 16 and 187 ± 8.4 μM, respectively), suggesting that the observed increase in ADI kinetics for whole-cell studies of *M. hominis*-infected *T. vaginalis* was due to the contribution of *M. hominis* and not overexpression of host cell ADI. Further purification of hydrogenosome-enriched fractions by Percoll gradients revealed a single fraction with maximum ADI activity from SS22 and an isopycnic density of 1.23 g ml^{-1} (Fig. 5a), which overlays malic enzyme, a marker for hydrogenosomes (Fig. 5c). When the hydrogenosome-enriched fraction obtained from SS22-MOZ2 was used, the Percoll gradient purification resulted in two fractions with ADI activity, the hydrogenosomal fraction at 1.24 g ml^{-1} and a second fraction at 1.27 g ml^{-1} (Fig. 5b). The activity in the 1.27 g ml^{-1} fraction overlaid *M. hominis* ADI (Fig. 5d).

Intracellular and extracellular amine concentrations from *T. vaginalis* SS22 and SS22-MOZ2 cultures

The intracellular and extracellular concentrations of amines associated with the ADH pathway were determined by HPLC analysis of acid extracts. The intracellular concentration of arginine was not significantly different in the two strains (Table 3). However, arginine utilization was approximately 2.5-fold increased in *T. vaginalis* (SS22-MOZ2) cultures infected with *M. hominis* (Table 3). The increased flow through the ADH pathway of *T. vaginalis* SS22-MOZ2 was reflected by the increased intracellular ornithine concentration, which was 15-fold higher in SS22-MOZ2 than in the

Table 2. Flux control coefficients for enzymes of the ADH pathway in *T. vaginalis* strain SS22 and *T. vaginalis* infected with *M. hominis* (SS22-MOZ2)

Enzyme elasticities and flux control coefficients are expressed as $\varepsilon^{Enzyme}_{substrate}$ and C^{J}_{Enzyme}, respectively.

T. vaginalis strain	ε^{ADI}_{arg}	ε^{OCT}_{cit}	ε^{ODC}_{orn}	C^{J}_{ADI}/C^{J}_{OCT}	C^{J}_{ADI}/C^{J}_{ODC}
SS22	1.07	1.01	0.04	0.94	0.035
SS22-MOZ2	1.00	0.98	0.09	0.98	0.10

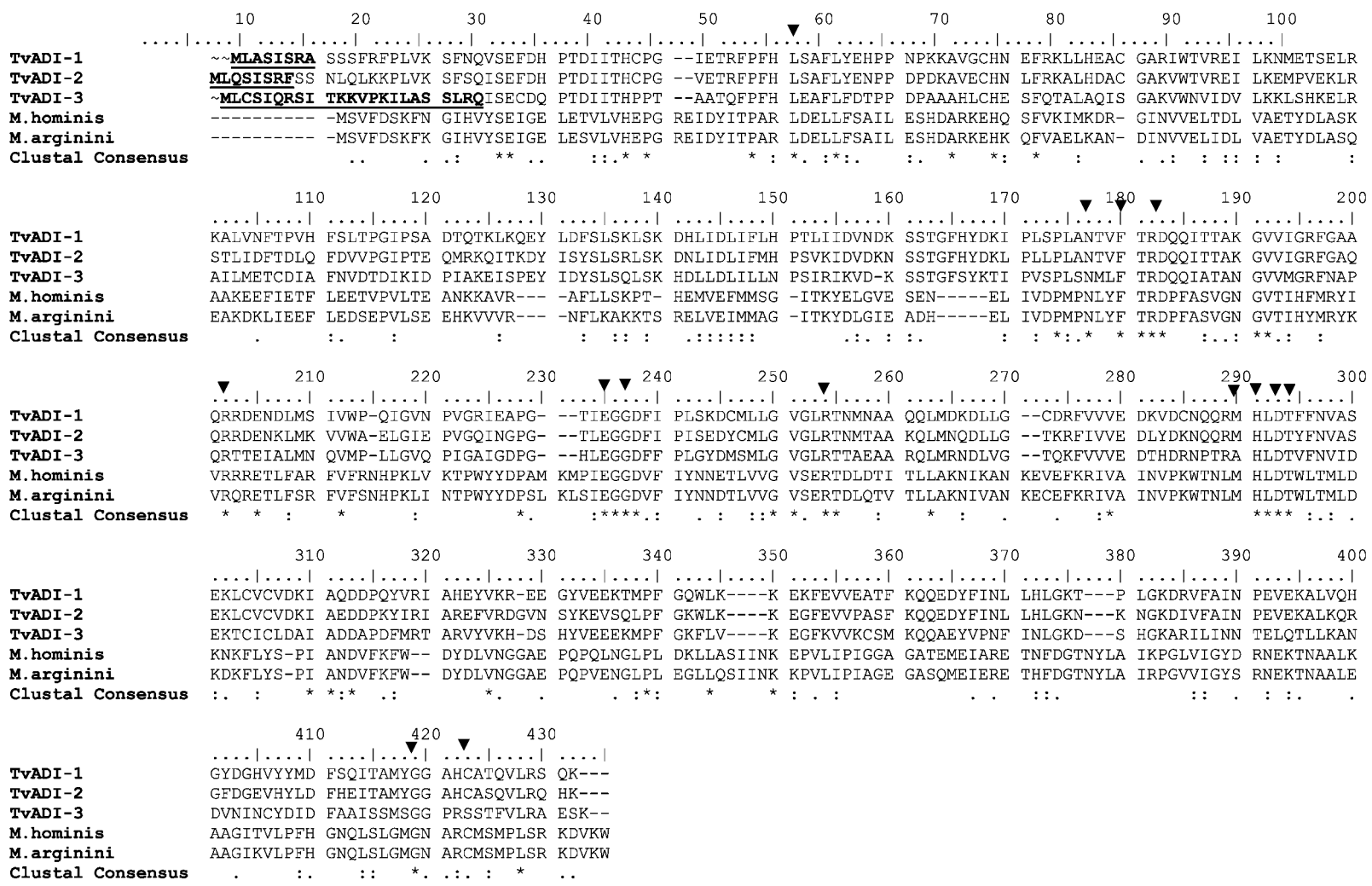

Fig. 3. Genome sequence of ADI from *T. vaginalis*. Sequences were obtained by BLAST search in the *T. vaginalis* genome database (strain G3) of Eukaryotic Pathogen Database Resources (http://eupathdb.org/eupathdb/) using *G. intestinalis* (strain WB) ADI (accession no. XP_001705755) as query. Three sequences with significant similarity to *G. intestinalis* ADI (TVAG_467820, TVAG_344520 and TVAG_183850) were aligned with *M. hominis* (accession no. D13314 0.1) and *M. arginini* (accession no. CAA38210) using CLUSTAL_X (Thompson *et al.*, 1997) and manually edited with BioEdit software (Hall, 1999). Putative mitochondrial targeting sequences (underlined) were predicted using the program PSORT II (http://psort.hgc.jp/). Triangles indicate residues involved in substrate binding and reaction mechanism (Das *et al.*, 2004). Asterisk, fully conserved residue; colon, 'strong' group; period, conserved 'weaker' group according to CLUSTAL X.

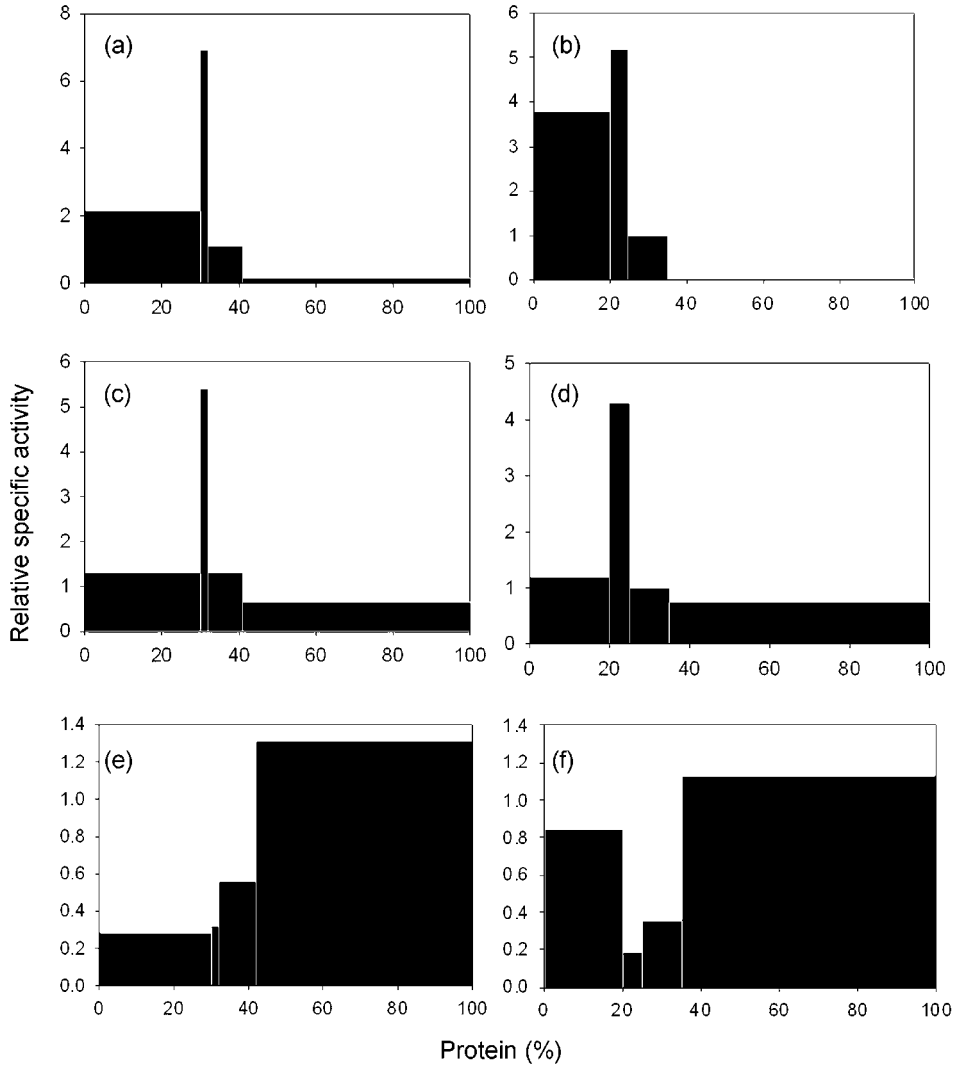

Fig. 4. Subcellular localization of ADH enzymes in *T. vaginalis* SS22, *T. vaginalis* infected with *M. hominis* (SS22-MOZ2) and *M. hominis* MOZ2. Distribution and percentage recovery for each enzyme after subcellular fractionation of *T. vaginalis* (a) SS22 malic enzyme, 93 %; (b) SS22-MOZ2 malic enzyme, 88 %; (c) SS22 ADI, 87 %; (d) SS22-MOZ2 ADI, 96 %; (e) SS22 cOCT, 98 %; and (f) SS22-MOZ2 cOCT, 104 %.

parent strain SS22 (Table 3). A similar fivefold increase was observed for the extracellular ornithine concentration. Also, intracellular and extracellular putrescine had approximately twofold higher intracellular and threefold higher extracellular concentrations in SS22-MOZ2 compared with the parent SS22. A duplicate set of data were obtained using the *T. vaginalis* C1/C1-MOZ2 pair (Supplementary Table S2).

RT-qPCR ADI in *M. hominis*-infected and -uninfected *T. vaginalis*

The ratio of mRNA expression levels for ADI in SS22-MOZ2/SS22 ($2^{-\Delta\Delta Ct}$ infected *T. vaginalis*/$2^{-\Delta\Delta Ct}$ uninfected *T. vaginalis*) was 0.69 (TvADI-1), 0.6 (TvADI-2) and 1.29 (TvADI-3). These results indicate that TvADI-1 and TvADI-2 are 30 % downregulated, while TvADI-3 is 30 % upregulated in mycoplasma-infected trichomonads. Since a 30 % difference in mRNA expression, as evaluated by real-time RT-qPCR, is considered minor, it is concluded that an absence of upregulation or downregulation of the overall TvADI expression occurs in *T. vaginalis* cells infected with *M. hominis*.

DISCUSSION

ADI is the first step in the most widespread anaerobic route of arginine degradation via the ADH pathway. The pathway provides an important source of energy generation from amino acids in the absence of oxygen in some protists (Schofield *et al.*, 1990; Yarlett *et al.*, 1996), and *T.*

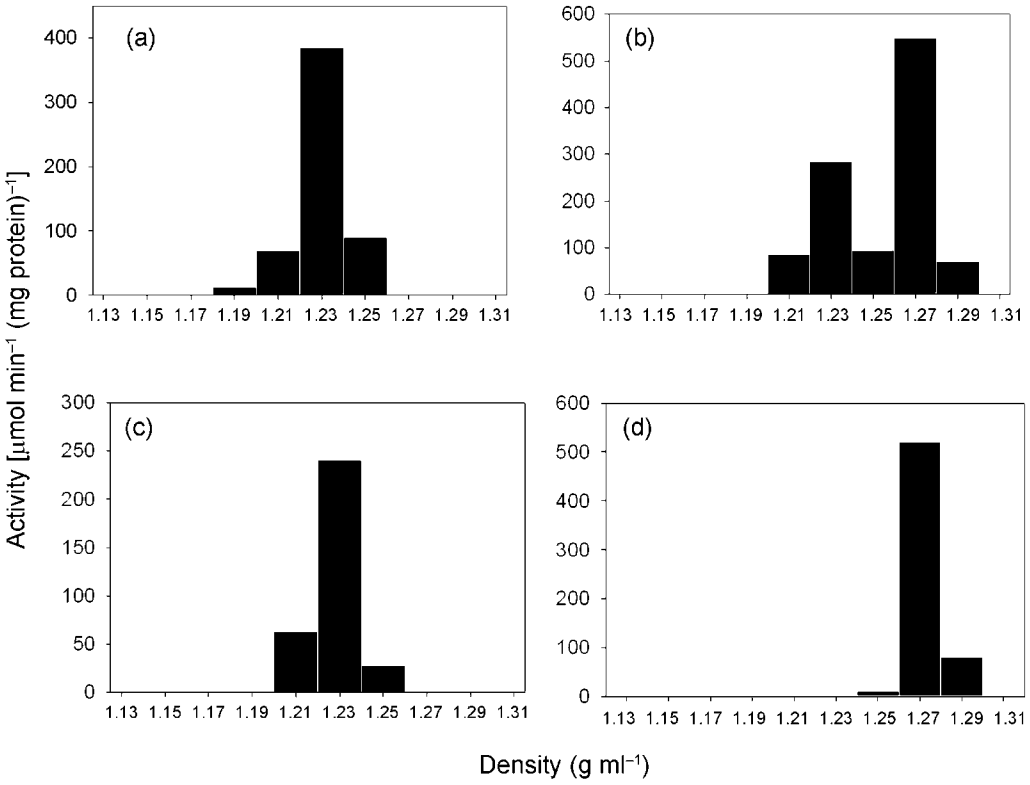

Fig. 5. Isopycnic density-gradient centrifugation of the hydrogenosome-enriched fractions. Hydrogenosome-enriched fractions from *T. vaginalis* SS22, *T. vaginalis* infected with *M. hominis* SS22-MOZ2 and *M. hominis* MOZ2 obtained by differential centrifugation were purified using Percoll gradients. Fractions were assayed for ADI and malic enzyme as described in Methods. (a) Distribution of ADI in SS22 revealed a major peak of activity at a density of 1.23 g ml^{-1}; (b) SS22-MOZ2 had two peaks of activity at densities of 1.23 and 1.27 g ml^{-1} for ADI; (c) SS22 had a single major peak of activity at 1.23 g ml^{-1} for the hydrogenosome marker enzyme malic enzyme; (d) MOZ2 had a single peak of activity for ADI at a density of 1.27 g ml^{-1}. Percentage recoveries were 84 and 81 % for ADI and malic enzyme, respectively, for *T. vaginalis* SS22; 86 % for ADI with SS22-MOZ2; 93 % for ADI with MOZ2.

vaginalis can potentially meet 10 % of its energy needs from this pathway (Yarlett *et al.*, 1996). The ADH pathway is also present in *M. hominis* (Fenske & Kenny, 1976), a member of the Mollicutes, which has a symbiotic relationship with *T. vaginalis* (Dessì *et al.*, 2005). Consequently, *T. vaginalis* infected with *M. hominis* contains two localized pathways competing for the same substrate, arginine. The effect of this endosymbiotic relationship on the ADH pathway of *T. vaginalis* has not previously been examined. We showed that cultures of *T. vaginalis* infected with *M. hominis* exhibit

Table 3. Intracellular and extracellular concentrations of amines in the parent uninfected *T. vaginalis* strain SS22 and *T. vaginalis* infected with *M. hominis* (SS22-MOZ2)

The concentration of amines was determined by HPLC as described in Methods.

Amine	*T. vaginalis* SS22		*T. vaginalis* SS22-MOZ2	
	Intracellular concentration (µM per 10^6 cells)	Extracellular concentration (mM)	Intracellular concentration (µM per 10^6 cells)	Extracellular concentration (mM)
Arginine	0.51	5.63	0.46	2.31
Citrulline	0.12	0.15	0.06	0.04
Ornithine	0.03	0.06	0.45	0.31
Putrescine	0.19	1.92	0.43	5.32

increased arginine consumption and a concomitant increase in ornithine and putrescine production. *M. hominis* has a minimal genome that lacks an ODC gene (Pereyre *et al.*, 2009) and ODC enzyme activity (this study); hence, it is likely that the ornithine produced by *M. hominis* is exported, possibly via an arginine/ornithine transporter, as demonstrated in other prokaryotes that contain the ADH pathway (Driessen *et al.*, 1987). *M. hominis* has a number of transporters that are capable of satisfying its nutritional requirement for several amino acids (Pereyre *et al.*, 2009). In particular, MHO_5040 is proposed to encode a functional *M. hominis* arginine permease (Pereyre *et al.*, 2009). The rapid removal of arginine from the cytoplasm of *T. vaginalis* by *M. hominis* and its replacement by exported ornithine via a putative arginine/ornithine transporter would result in an increased cytoplasmic ornithine concentration, which could then drive increased putrescine formation by the *T. vaginalis* ODC. Thus, this relationship would provide *M. hominis* with a constant supply of putrescine, which it is incapable of synthesizing. The benefit of this symbiotic relationship to *T. vaginalis* is not so clear; however, the increased scavenging of arginine may be significant, since it would reduce the amount of free arginine available for nitric oxide (NO) production by host macrophages. *T. vaginalis* has a flavorubredoxin-like-dependent NO reductase with a reported K_m of 1.2 μM, which would effectively remove NO (Sarti *et al.*, 2004). However, the concentration of arginine in vaginal fluid has been reported to be 210 μM (Chen *et al.*, 1982), which is reduced to undetectable levels during infection; hence, the combined arginine sink in *T. vaginalis* infected with *M. hominis* would effectively reduce free arginine concentrations to levels below the K_m of the host NO synthase. Depletion of arginine by ADI could therefore block NO production by macrophages and thereby block an important host defence mechanism (Dillon *et al.*, 2002). A role for *M. hominis* ADI in suppression of NO production caused by macrophage-inducible NO synthase has been proposed (Noh *et al.*, 2002). It has been proposed that *G. intestinalis* releases ADI in contact with host epithelial cells, which protects it from host NO production (Ringqvist *et al.*, 2008). The *G. intestinalis* ADI has also been implicated in multiple functions, including antigenic switching and migration to the nucleus, where it has a regulatory role in gene expression during encystation (Touz *et al.*, 2008). In *T. vaginalis*, however, ADI localizes predominantly to the hydrogenosomal fraction.

We have previously demonstrated that ADI is the step with the lowest velocity and is therefore proposed to be the rate-limiting step of the pathway (Yarlett *et al.*, 1996). However, the actual change in flow through the pathway caused by the presence of *M. hominis* is more complex than this, and is best described by determination of the flux control coefficients and elasticity of the enzymes involved (Fell, 1997). Based on the kinetic data for the ADH enzymes and knowing the intracellular concentrations of the intermediates, the elasticity of each enzyme of the pathway can be determined (Table 2). From this it can be shown that the increase in ornithine has a significant effect upon the flux control of the pathway (C^J_{ODC} increases from 1/25 to 1/10). Based upon the data obtained in this study we propose that the additional ornithine present in the *T. vaginalis* cytosol is derived from *M. hominis*. Ornithine drives the formation of putrescine via a *T. vaginalis* ODC and can also be a substrate for the *T. vaginalis* lysine/ornithine aminotransferase (OAT; EC 2.6.1.13; *TVAG* 258770; Carlton *et al.*, 2007), resulting in the formation of glutamate and Δ-pyrroline 5-carboxylate (Lowe & Rowe, 1986; Carlton *et al.*, 2007). Glutamate, in turn, could drive the formation of cytosolic alanine by alanine aminotransferase (EC 2.6.1.2; Lowe & Rowe, 1986). Multiple copies of the alanine aminotransferase gene have been identified in the *T. vaginalis* genome (Carlton *et al.*, 2007); based upon the presence of a hydrogenosomal targeting sequence, these genes encode alanine aminotransferases that localize to both the hydrogenosome and the cytosol (Carlton *et al.*, 2007). The cytosolic alanine can enter the hydrogenosome, resulting in the production of hydrogenosomal pyruvate, and could therefore act as an alanine/pyruvate shuttle for provision of hydrogenosomal pyruvate and be involved in ATP generation by the *T. vaginalis* pyruvate : ferredoxin oxidoreductase-coupled succinate thiokinase pathway. We conclude that the association of *M. hominis* with *T. vaginalis* is an example of a mutually beneficial endosymbiotic relationship.

ACKNOWLEDGEMENTS

The authors thank Dr Thomas E. Gorrell for helpful suggestions. Parts of this study were supported by grants from the National Institutes of Health National Institute for Allergy and Infectious Diseases (NIH-NIAID) 49785 (N. Y.), and the Academy of Science of the Czech Republic IAA501110631 and MSM0021620858 (J. T.).

REFERENCES

Blanchard, A., Yanez, A., Dybvyg, K., Watson, H. L., Griffiths, G. & Cassel, G. H. (1993). Evaluation of intraspecies genetic variation within the 16S rRNA gene of *M. hominis* and detection by PCR. *J Clin Microbiol* **31**, 1358–1361.

Boyde, T. R. & Rahmatullah, M. (1980). Optimization of conditions for the colorimetric determination of citrulline, using diacetyl monoxime. *Anal Biochem* **107**, 424–431.

Carlton, J. M., Hirt, R. P., Silva, J. C., Delcher, A. L., Schatz, M., Zhao, Q., Wortman, J. R., Bidwell, S. L., Alsmark, U. C. & other authors (2007). Draft genome sequence of the sexually transmitted pathogen *Trichomonas vaginalis*. *Science* **315**, 207–212.

Chen, K. C., Amsel, R., Eschenbach, D. A. & Holmes, K. K. (1982). Biochemical determination of vaginitis: determination of diamines in vaginal fluid. *J Infect Dis* **145**, 337–345.

Cornish-Bowden, A. (2004). *Fundamentals of Enzyme Kinetics*, 3rd edn. London: Portland Press.

Das, K., Butler, G. H., Kwiatkowski, V., Clark, A. D., Jr, Yadav, P. & Arnold, E. (2004). Crystal structure of arginine deiminase with covalent reaction intermediates; implications for catalytic mechanism. *Structure* **12**, 657–667.

Dessì, D., Delogu, G., Emonte, E., Catania, M. R., Fiori, P. L. & Rappelli, P. (2005). Long-term survival and intracellular replication of *Mycoplasma hominis* in *Trichomonas vaginalis* cells: potential role of the protozoon in transmitting bacterial infection. *Infect Immun* **73**, 1180–1186.

Diamond, L. S. (1957). The establishment of various trichomonads of animals and man in axenic cultures. *J Parasitol* **43**, 488–490.

Dillon, B. J., Holtsberg, F. W., Ensor, C. M., Bomalaski, J. S. & Clark, M. A. (2002). Biochemical characterization of the arginine degrading enzymes arginase and arginine deiminase and their effect on nitric oxide production. *Med Sci Monit* **8**, BR248–BR253.

Dolezal, P., Vánacová, S., Tachezy, J. & Hrdy, I. (2004). Malic enzymes of *Trichomonas vaginalis*: two enzyme families, two distinct origins. *Gene* **329**, 81–92.

Driessen, A. J., Poolman, B., Kiewiet, R. & Konings, W. (1987). Arginine transport in *Streptococcus lactis* is catalyzed by a cationic exchanger. *Proc Natl Acad Sci U S A* **84**, 6093–6097.

Fell, D. (1997). Measuring control coefficients. In *Frontiers in Metabolism 2: Understanding the Control of Metabolism*, pp. 135–195. Edited by K. Snell. London: Portland Press.

Fenske, J. D. & Kenny, G. E. (1976). Role of arginine deiminase in growth of *Mycoplasma hominis*. *J Bacteriol* **126**, 501–510.

Griswold, A., Chen, Y. Y., Snyder, J. A. & Burne, R. A. (2004). Characterization of the arginine deiminase operon in *Streptococcus rattus* FA-1. *Appl Environ Microbiol* **70**, 1321–1327.

Hall, T. A. (1999). BioEdit: a user-friendly biological sequence alignment editor and analysis program for Windows 95/98/NT. *Nucleic Acids Symp Ser* **41**, 95–98.

Linstead, D. & Cranshaw, M. A. (1983). The pathway of arginine catabolism in the parasitic flagellate *Trichomonas vaginalis*. *Mol Biochem Parasitol* **8**, 241–252.

Lowe, P. N. & Rowe, A. F. (1986). Aminotransferase activity in *Trichomonas vaginalis*. *Mol Biochem Parasitol* **21**, 65–74.

Lu, X., Galkin, A., Herzberg, O. & Dunaway-Mariano, D. (2004). Arginine deiminase uses an active-site cysteine in nucleophilic catalysis of L-arginine hydrolysis. *J Am Chem Soc* **126**, 5374–5375.

Noh, E. J., Kang, S. W., Shin, Y. J., Kim, D. C., Park, I. S., Kim, M. Y., Chun, B. G. & Min, B. H. (2002). Characterization of *Mycoplasma* arginine deiminase expressed in *E. coli* and inhibitory regulation of nitric oxide synthesis. *Mol Cells* **13**, 137–143.

Pereyre, S., Sirand-Pugnet, P., Bevan, L., Charron, A., Renaudin, H., Barre, A., Avenaud, P., Jacob, D., Couloux, A. & other authors (2009). Life on arginine for *Mycoplasma hominis*. Clues from its minimal genome and comparison with other human urogenital mycoplasmas. *PLoS Genet* **5**, e1000677.

Rappelli, P., Addis, M. F., Carta, F. & Fiori, P. L. (1998). *Mycoplasma hominis* parasitism of *Trichomonas vaginalis*. *Lancet* **352**, 1286.

Ringqvist, E., Palm, J. E., Skarin, H., Hehl, A. B., Weiland, M., Davids, B. J., Reiner, D. S., Griffiths, W. J., Eckmann, L. & other authors (2008). Release of metabolic enzymes by *Giardia* in response to interaction with intestinal epithelial cells. *Mol Biochem Parasitol* **159**, 85–91.

Sarti, P., Fiori, P. L., Forte, E., Rappelli, P., Teixeira, M., Mastronicola, D., Sanciu, G., Giuffrè, A. & Brunori, M. (2004). *Trichomonas vaginalis* degrades nitric oxide and expresses a flavorubredoxin-like protein: a new pathogenic mechanism? *Cell Mol Life Sci* **61**, 618–623.

Schofield, P. J., Costello, M., Edwards, M. R. & O'Sullivan, W. J. (1990). The arginine dihydrolase pathway is present in *Giardia intestinalis*. *Int J Parasitol* **20**, 697–699.

Stamatakis, A. (2006). RAxML-VI-HPC: maximum likelihood-based phylogenetic analyses with thousands of taxa and mixed models. *Bioinformatics* **22**, 2688–2690.

Swofford, D. L. (1998). Phylogenetic analysis using parsimony (PAUP), version 4. Sunderland, MA: Sinauer Associates.

Thompson, J. D., Gibson, T. J., Plewniak, F., Jeanmougin, F. & Higgins, D. G. (1997). The CLUSTAL_X windows interface: flexible strategies for multiple sequence alignment aided by quality analysis tools. *Nucleic Acids Res* **25**, 4876–4882.

Touz, M. C., Ropolo, A. S., Rivero, M. R., Vranych, C. V., Conrad, J. T., Svard, S. G. & Nash, T. E. (2008). Arginine deiminase has multiple regulatory roles in the biology of *Giardia lamblia*. *J Cell Sci* **121**, 2930–2938.

Yarlett, N., Goldberg, B., Moharrami, M. A. & Bacchi, C. J. (1993). *Trichomonas vaginalis*: characterization of ornithine decarboxylase. *Biochem J* **293**, 487–493.

Yarlett, N., Lindmark, D. G., Goldberg, B., Moharrami, M. A. & Bacchi, C. J. (1994). Subcellular localization of the enzymes of the arginine dihydrolase pathway in *Trichomonas vaginalis* and *Tritrichomonas foetus*. *J Eukaryot Microbiol* **41**, 554–559.

Yarlett, N., Martinez, M. P., Moharrami, M. A. & Tachezy, J. (1996). The contribution of the arginine dihydrolase pathway to energy metabolism by *Trichomonas vaginalis*. *Mol Biochem Parasitol* **78**, 117–125.

Edited by: C. Citti